Responses to Comments and Suggestions of Reviewer #2

Ref. No.: egusphere-2026-361

Title: Ecosystem Climate Sensitivities Drive the Divergence in Aerosol-Induced Carbon Uptake Across CMIP6 Models

Corresponding author: Prof. Zhaoyang Zhang

The authors analyze CMIP6 simulations regarding the GPP response to aerosol emissions and present a neat decomposition framework to identify the major differences between the modelled responses. The study highlights an important aspect regarding the importance of vegetation dynamics and responses in driving global carbon dynamics, climate interactions, and differences in model projections. As such, the study is very well suited for publication in GMD. However, there are several aspects that require more thorough discussion and methodological explanation before the paper can be published.

Response: We sincerely thank the reviewer for the positive and encouraging evaluation of our manuscript. We also appreciate your highly constructive feedback. We completely agree that the manuscript would greatly benefit from more thorough discussion and clearer methodological explanations. We have carefully considered all of your suggestions and have made substantial revisions to the manuscript. Changes in the revised manuscript are highlighted with Yellow color. Our responses are provided below (words in **Blue** is the responses and in **Red** is the context of revised paper).

General comments:

1. The derivation of the attribution framework should be explained in more detail. Could you provide a rational for your steps of using a first-order Taylor expansion and how eq (2) is derived (might be worth writing it similar to eq. 4 first)? Is it equivalent to the total differential? Is there a methodological reason that prevents you from explicitly testing variation in fPAR? And does fitting the regression per PFT remove the fPAR in eq. 6?

Response: Thanks for your comments and suggestions. We agree that the mathematical derivation and its underlying biophysical assumptions need to be stated more clearly. We have expanded the derivation in Section 2.3 of the revised manuscript to address all the questions. Yes, the reviewer is entirely correct. The first-order Taylor expansion we applied to Equation 1 is mathematically equivalent to the total differential for a multi-variable function. We have modified the following equations according to the suggestions of the reviewer. (Please see Line 172-178).

"

Equation 2 can be rewritten as

$$\boldsymbol{\delta GPP \approx (fPAR * LUE) * \delta PAR + (PAR * LUE) * \delta fPAR + (PAR * fPAR) * \delta LUE} \quad (3)$$

Bloomfield et al. (2022) showed that a generalized linear mixed- effects model could well represent the response of LUE to environmental factors. In addition, aerosol-induced changes in climatic variables are small. Therefore, the change in LUE ($\boldsymbol{\delta LUE}$) can be approximated linearly:

$$\boldsymbol{\delta LUE \approx \frac{\partial LUE}{\partial tas}\delta tas + \frac{\partial LUE}{\partial pr}\delta pr + \frac{\partial LUE}{\partial CI}\delta CI} \quad (4)$$

Substituting Equation (4) into Equation (3) can get the full decomposition:

$$\boldsymbol{\delta GPP \approx fPAR * LUE * \delta PAR + PAR * LUE * \delta fPAR + \frac{\partial LUE}{\partial tas} * fPAR * PAR * \delta tas + \frac{\partial LUE}{\partial pr} * fPAR * PAR * \delta pr + \frac{\partial LUE}{\partial CI} * fPAR * PAR * \delta CI} \quad (5)$$

A multivariate regression model was constructed for specific plant functional type (PFT) and ESM to capture the impacts of climatic drivers and systematic model biases. The regression equation for a specific model (m) is defined as:

$$\boldsymbol{\delta GPP_m \approx \beta_{0,m} + \beta_{1,m}\delta PAR_m + \beta_{f,m}PAR_{clim} * \delta fPAR_m + \beta_{2,m}PAR_{clim} * \delta tas_m + \beta_{3,m}PAR_{clim} * \delta pr_m + \beta_{4,m}PAR_{clim} * \delta CI_m} \quad (6)$$

Here, $\boldsymbol{\delta GPP_m}$ represents the aerosol-induced anomaly of GPP (Historical-Hist-piAer) from model $\boldsymbol{m}$. $\boldsymbol{PAR_{clim}}$ is the climatological baseline PAR (0.45*rads). $\boldsymbol{\beta_1}$ is the product of fPAR and LUE, while $\boldsymbol{\beta_f}$ represents the baseline LUE. $\boldsymbol{\beta_{2-4}}$ represents

the product of fPAR and the partial derivatives of LUE to climatic factors, while the intercept $\boldsymbol{\beta_0}$ represents the systematic bias of the model. To address multicollinearity, standardized ridge regression was used for the specific PFT.

To quantify the inter-model divergence, we calculated the deviation of model $\boldsymbol{m}$ from the multi-model ensemble mean (mmm) by using the Equation 7.

$$\Delta(\boldsymbol{\delta GPP}) = \boldsymbol{\delta GPP_m} - \boldsymbol{\delta GPP_{mmm}} \quad (7)$$

By substituting the regression equations into Equation 7 and rearranging terms, we derived the final equation:

$$\Delta(\boldsymbol{\delta GPP}) = \underbrace{\sum_i \boldsymbol{\beta_{i,mmm}}\left(\boldsymbol{X_{i,m}} - \boldsymbol{X_{i,mmm}}\right)}_{\textit{State contribution}} + \underbrace{\sum_i \boldsymbol{X_{i.m}}\left(\boldsymbol{\beta_{i,m}} - \boldsymbol{\beta_{i,mmm}}\right) + \left(\boldsymbol{\beta_{f,m}}\boldsymbol{X_{f,m}} - \boldsymbol{\beta_{f,mmm}}\boldsymbol{X_{f,m}}\right) + \left(\boldsymbol{\beta_{0,m}} - \boldsymbol{\beta_{0,mmm}}\right)}_{\textit{Sensitivity contribution}} \quad (8)$$

where $\boldsymbol{X_i}$ represents the independent variables (including interaction terms). This equation decomposes the model spread into two components:

(1) State contribution: The divergence arising from differences in the simulated aerosol radiative and climatic effects (e.g., differences in simulated pr: $\boldsymbol{X_{i,m}} - \boldsymbol{X_{i,mmm}}$), weighted by the mean pr sensitivity ($\boldsymbol{\beta_{i,mmm}}$).

(2) Sensitivity contribution: The divergence arising from ecosystem climate sensitivities across ESMs. This term represents the contributions from dynamic photosynthesis sensitivity differences ($\boldsymbol{\beta_{i,m}} - \boldsymbol{\beta_{i,mmm}}$), structural feedback divergence driven by LAI simulations ($\boldsymbol{\beta_{f,m}}\boldsymbol{X_{f,m}} - \boldsymbol{\beta_{f,mmm}}\boldsymbol{X_{f,m}}$) and the systematic bias differences ($\boldsymbol{\beta_{0,m}} - \boldsymbol{\beta_{0,mmm}}$).

”

In the previous version of the paper, we assumed that $\delta fPAR$ is equal to 0. Because previous studies have shown that the diffuse fertilization effect (DFE) induced by aerosols is primarily driven by improved light-use efficiency (LUE) rather than by changes in light absorption (fPAR) (Shao et al., 2020; Zhang et al., 2024). However, fPAR is affected not only by diffuse radiation, but also by vegetation canopy structure, which is further modulated by aerosol climatic effects. Therefore, we modified the Equation 2-8 to consider the impacts of fPAR.

We have considered the impacts of fPAR according to the reviewer's suggestion.

2. The authors state that there are large differences in the ecosystem response to the climatic changes (e.g., photosynthesis to temperature), but could expand in the discussion on the underlying drivers of these differences between vegetation models and how they relate to the observed differences in sensitivities. They do state differences between the vegetation models (e.g., L462-489), but they do not necessarily relate how these differences match with the observed sensitivity differences. Beyond discussion, one way of doing this might be to show how the model fits vary between different PFTs across models. Another suggestion, is it possible to do the analysis spatially and for each year, rather than through time?

Response: Thanks for your highly constructive and insightful suggestions. We agreed that it was essential to link the differences among models in the discussion with the observed sensitivity differences. We added some sentences in the discussion (Please see Line 471-472, 479-480, 487-489, 499, 513-517) and listed the empirical sensitivities (β) for each PFT derived from our attribution framework. (Please see Table S2-S6 in Supplementary Materials). According to the suggestions, we also added the spatial distribution of sensitivity contribution and state contribution for each model. However, we did not analyze the contribution for each year. Because the aerosol-induced annual anomalies of GPP are relatively weak, the results for each year are significantly influenced by noise. (Please see Figure S9). We also add some sentences to illustrate the spatial pattern of state and sensitivity contributions. (Please see Line 426-436).

"The sensitivity coefficients for CI from UKESM1-0-LL are lowest in 8 out 11 PFTs (Table S6).

Table S6 shows that sensitivity coefficients for CI from IPSL-CM6A-LR approach zero across almost all PFTs.

However, our results showed that there were large differences in the temperature sensitivities (β_{tas}) and structural feedbacks (fPAR) across different PFTs (Table S3 and S4).

These divergent responses are captured by the β_{Tas} values (Table S4).

Our results are fully consistent with the theory. Table S3 showed that the structural feedback of BCC-ESM1 is generally the highest among all ESMs across almost all PFTs. This suggests that heat-accumulation phenology scheme of BCC-ESM1 makes the vegetation phenology more sensitive to temperature changes induced by aerosols."

"Table S2: Sensitivity Coefficients for Total Radiation (β_{Rsds}) per Plant Functional Type (PFT). ENF, Evergreen Needleleaf Forest; EBF, Evergreen Broadleaf Forest; DBF, Deciduous Broadleaf Forest; MF, Mixed Forest; OSH, Open Shrublands; WSA, Woody Savannas; SAV, Savannas; GRA, Grasslands; WET, Wetlands; CRO, Croplands; BAR, Barren or Sparsely Vegetated.

PFT	BCC-ESM1	IPSL-CM6A-LR	MPI-ESM-1-2-HAM	NorESM2-LM	UKESM1-0-LL
ENF	0.060004	-0.009846	0.099274	0.070613	-0.000013
EBF	0.015620	0.041606	-0.087938	-0.037287	-0.112900
DBF	0.024524	0.016964	0.031943	0.043793	0.054809
MF	0.078144	0.017688	0.085544	0.042982	0.127988
OSH	0.029205	0.016505	0.032895	0.030918	0.067173
WSA	0.045420	0.002403	0.075611	0.032405	0.105841
SAV	0.043868	0.015162	0.080874	0.005151	0.114596
GRA	0.024818	0.001811	0.045616	0.010737	0.072748
WET	0.009624	0.013132	0.052078	0.021471	0.177116
CRO	0.017304	-0.008540	0.066934	0.020178	0.055000
BAR	-0.003314	0.000968	0.005285	0.007699	0.046106

Table S3: Sensitivity Coefficients for Canopy Structure ($\boldsymbol{\beta_{fPAR}}$) per Plant Functional Type (PFT). ENF, Evergreen Needleleaf Forest; EBF, Evergreen Broadleaf Forest; DBF, Deciduous Broadleaf Forest; MF, Mixed Forest; OSH, Open Shrublands; WSA, Woody Savannas; SAV, Savannas; GRA, Grasslands; WET, Wetlands; CRO, Croplands; BAR, Barren or Sparsely Vegetated.

PFT	BCC-ESM1	IPSL-CM6A-LR	MPI-ESM-1-2-HAM	NorESM2-LM	UKESM1-0-LL
ENF	0.114436	0.024338	0.006533	0.033213	0.061316
EBF	0.052473	0.075333	0.032322	0.057174	0.031813
DBF	0.078090	0.040978	0.079064	0.031206	-0.045522
MF	0.069046	0.031780	0.029651	0.035106	0.021965
OSH	0.038614	0.024632	0.007610	0.038204	0.012023
WSA	0.085676	0.026879	0.023365	0.029852	0.013253
SAV	0.051983	0.029588	0.023297	0.029316	0.026310
GRA	0.042318	0.025701	0.010717	0.023344	0.015249
WET	0.102288	0.031689	0.046637	0.031017	0.034506
CRO	0.030129	0.034112	0.029883	0.024567	0.007116
BAR	0.024839	0.021880	0.004078	0.010107	0.003583

Table S4: Sensitivity Coefficients for Temperature ($\boldsymbol{\beta_{Tas}}$) per Plant Functional Type (PFT). ENF, Evergreen Needleleaf Forest; EBF, Evergreen Broadleaf Forest; DBF, Deciduous Broadleaf Forest; MF, Mixed Forest; OSH, Open Shrublands; WSA, Woody Savannas; SAV, Savannas; GRA, Grasslands; WET, Wetlands; CRO, Croplands; BAR, Barren or Sparsely Vegetated.

PFT	BCC-ESM1	IPSL-CM6A-LR	MPI-ESM-1-2-HAM	NorESM2-LM	UKESM1-0-LL
ENF	-0.002190	0.000240	-0.001651	0.000182	0.001585

PFT	BCC-ESM1	IPSL-CM6A-LR	MPI-ESM-1-2-HAM	NorESM2-LM	UKESM1-0-LL
EBF	0.001295	-0.000456	-0.003084	-0.000612	-0.003118
DBF	-0.000878	-0.000147	0.000666	-0.000001	0.001457
MF	-0.000185	-0.000032	-0.001440	-0.000465	-0.000310
OSH	0.000757	0.000585	0.000048	-0.000117	0.000593
WSA	-0.000888	0.000096	-0.000827	-0.000381	0.000434
SAV	0.000288	0.000038	-0.000311	-0.000540	0.001013
GRA	-0.000190	-0.000098	-0.000280	-0.000139	0.000120
WET	-0.000512	-0.000598	-0.000310	0.000095	0.000603
CRO	-0.000013	0.000312	-0.000921	-0.000161	0.000144
BAR	0.000048	-0.000008	0.000094	-0.000016	-0.000158

Table S5: Sensitivity Coefficients for Precipitation ($\boldsymbol{\beta_{Pr}}$) per Plant Functional Type (PFT). ENF, Evergreen Needleleaf Forest; EBF, Evergreen Broadleaf Forest; DBF, Deciduous Broadleaf Forest; MF, Mixed Forest; OSH, Open Shrublands; WSA, Woody Savannas; SAV, Savannas; GRA, Grasslands; WET, Wetlands; CRO, Croplands; BAR, Barren or Sparsely Vegetated.

PFT	BCC-ESM1	IPSL-CM6A-LR	MPI-ESM-1-2-HAM	NorESM2-LM	UKESM1-0-LL
ENF	6.2364	-43.3238	225.1848	-201.5129	603.2267
EBF	165.3611	65.0377	109.1002	-6.1268	179.2539
DBF	235.2866	87.0353	235.4413	134.8818	554.0208
MF	78.9363	69.4605	178.7551	5.2673	439.8855
OSH	-136.0682	-21.2328	409.4631	70.6018	203.1865
WSA	-12.3793	68.3307	206.0095	-5.8931	444.5251
SAV	-16.7918	13.2379	260.7474	59.1503	293.8231

PFT	BCC-ESM1	IPSL-CM6A-LR	MPI-ESM-1-2-HAM	NorESM2-LM	UKESM1-0-LL
GRA	-61.7907	3.3118	357.4310	96.3369	264.5849
WET	-178.3743	-189.3849	-268.0948	-20.6870	169.6031
CRO	-23.3069	-19.1447	292.8703	36.4451	376.3037
BAR	-16.1049	-14.4027	257.5394	81.6666	473.4937

Table S6: Sensitivity Coefficients for Clearness Index ($\boldsymbol{\beta_{CI}}$) per Plant Functional Type (PFT). ENF, Evergreen Needleleaf Forest; EBF, Evergreen Broadleaf Forest; DBF, Deciduous Broadleaf Forest; MF, Mixed Forest; OSH, Open Shrublands; WSA, Woody Savannas; SAV, Savannas; GRA, Grasslands; WET, Wetlands; CRO, Croplands; BAR, Barren or Sparsely Vegetated.

PFT	BCC-ESM1	IPSL-CM6A-LR	MPI-ESM-1-2-HAM	NorESM2-LM	UKESM1-0-LL
ENF	-0.179400	-0.004691	-0.133819	-0.159882	-0.059526
EBF	-0.034866	-0.037444	0.212178	0.068153	0.255530
DBF	-0.065590	-0.000442	-0.043122	-0.085349	-0.088917
MF	-0.197453	-0.023796	-0.122750	-0.081399	-0.251073
OSH	-0.096439	-0.031949	-0.068272	-0.044959	-0.200439
WSA	-0.131831	0.015233	-0.108264	-0.061041	-0.223069
SAV	-0.128428	-0.013374	-0.133998	0.006582	-0.227113
GRA	-0.058220	0.003497	-0.069130	-0.008668	-0.106475
WET	-0.049906	-0.059406	-0.018018	-0.036812	-0.294887
CRO	-0.074630	0.012429	-0.095520	-0.043673	-0.093012
BAR	0.002708	-0.001309	-0.007610	-0.007820	-0.043406

”

“

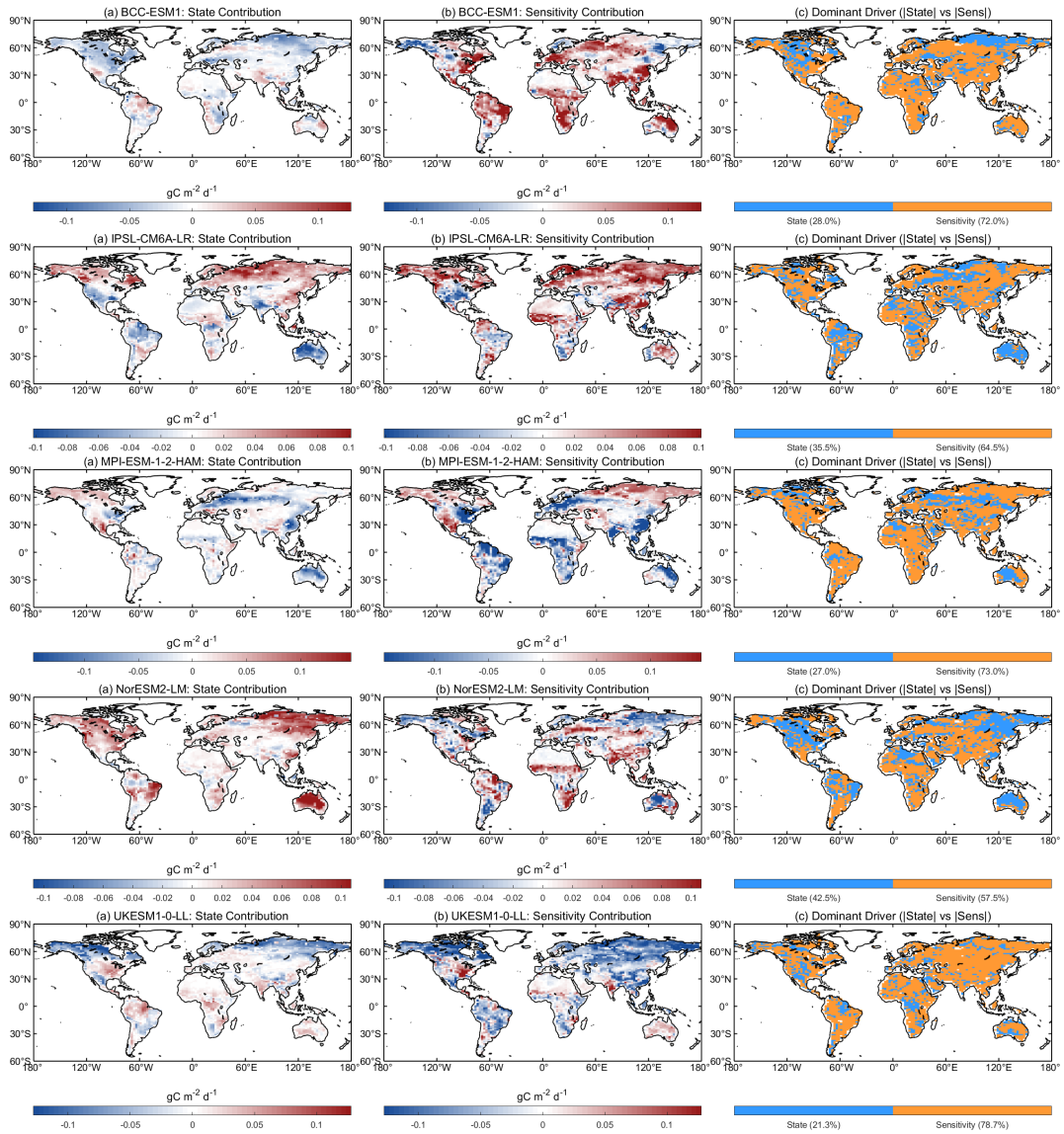

Figure S9. The spatial pattern of sensitivity contribution and state contribution and dominant driver across Earth System Models (ESMs). ”

“To analyze the spatial distribution of dominant driver governing the inter-model spread in aerosol-induced GPP anomalies, we showed the state and sensitivity contributions onto the global spatial grid (Figure S9). The results from spatial distribution further confirmed that the sensitivity contribution is the primary driver of GPP anomalies induced by aerosols. The contribution of ecosystem climate sensitivities ranges from 57.5% in NorESM2-LM to 78.7% in UKESM1-0-LL. Although the primary driver for each model is the sensitivity contribution, the spatial maps reveal significant inter-model divergence in the directionality of the sensitivities. MPI-ESM-1-2-HAM and UKESM1-0-LL show widespread negative sensitivity contributions in

most regions, while BCC-ESM1, MPI-ESM-1-2-HAM, and UKESM1-0-LL exhibit widespread negative state contributions in most regions. ”

3. The authors state that their framework captures >40% of the differences in the intermodal spread. A discussion of what the remaining variation represents is necessary.

Response: Thanks for your comments. We have updated the framework and now the framework can explain more than 50% of the inter-model spreads. We agreed that it was essential to explain remaining variation. We have added the underlying sources of this remaining variation. (Please see Line 520-529)

“Although the attribution framework in this study can capture more than 50% of inter-model GPP spreads, there are still large remaining unexplained variations. First, the framework omits higher-order non-linear climate interactions. For example, heatwaves accompanied by concurrent precipitation deficits exert an exponentially influence on VPD and vegetation stomatal conductance (Wang et al., 2025). Second, we utilized precipitation as the primary hydrological driver. However, precipitation might not adequately reflect the actual water stress on vegetation photosynthesis in some regions (Song et al., 2022). Third, the unexplained inter-model spread is highly related to unaccounted biogeochemical constraints, particularly the nutrition limitations in the model.

”

Detailed comments:

1. Introduction: Could you state what are the main aerosols and aerosol drivers during the considered period?

Response: Thanks for your comments. Hist-piAer experiment is run in parallel with the historical experiment but fixes the anthropogenic aerosol emissions at pre-industrial levels. Therefore, only anthropogenic aerosol was analyzed in this study. We have added some sentences to state the main aerosols and aerosol drivers during the study period. (Please see Line 107-110)

"During the 1850-2014 period, the main anthropogenic aerosols simulated by CMIP6 models are Sulfate, Organic Carbon (OC), and Black Carbon (BC) (Zhang et al., 2022). The variations of anthropogenic aerosols are driven by anthropogenic and biomass burning emissions."

2. L171. Please provide a definition of what δGPP represents and how it is derived from the available simulations. Also, it might help the reader to state at what time resolution you do this decomposition? E.g., the difference in GPP across the entire period 1850-2014 as derived from model and multi-model mean.

Response: Thanks for your comments. We have added the definition of δGPP and how it is derived. (Please see Line 177-179)

"δGPP is the mean difference in GPP induced by anthropogenic aerosols during 1850-2014 and can be calculated by subtracting the GPP of hist-piAer from that of historical for each ESM."

3. L211 and Fig. 1: Could you specify what time period this represents. Also, I would suggest to change the colour scheme, with red indicating loss and blue gain (even more intuitive would probably be a green-brown colour scale).

Response: Thanks for your comments. We have added the time period and replotted Figure 1 and Figure S5-S8. (Please see Line 221, Figure 1 and Figure S5-S8)

"

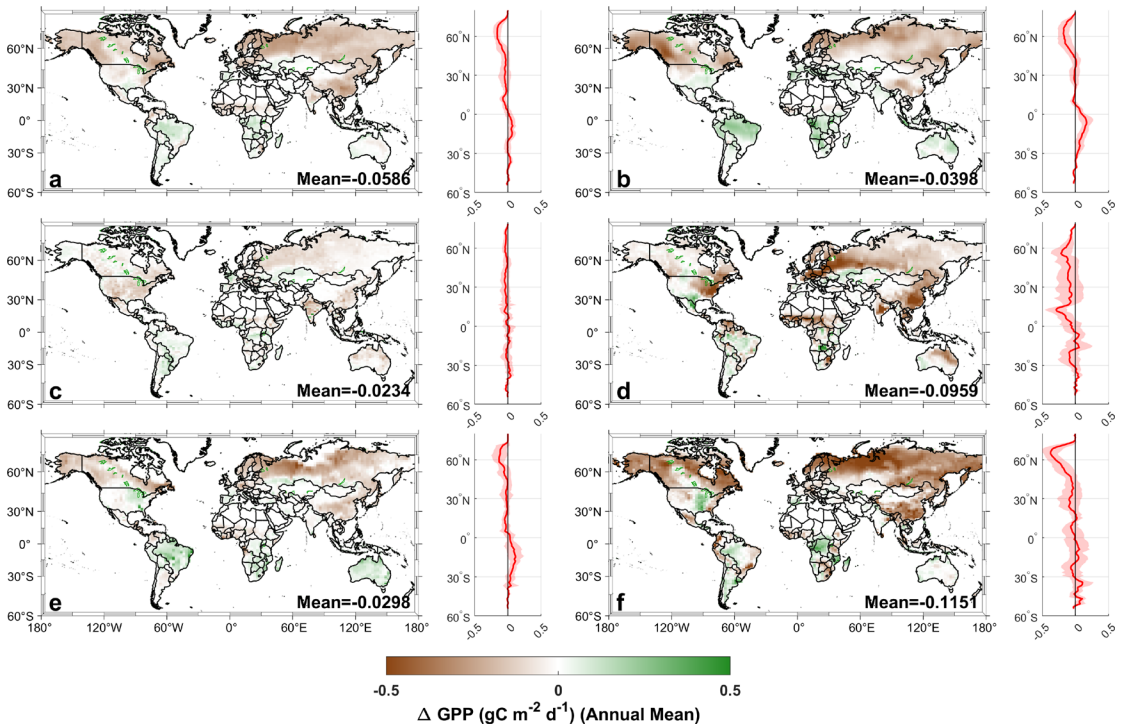

Figure 1. The spatial pattern of changes in ecosystem GPP (gC/(m^2d)) induced by aerosols from CMIP6 models (a. multi-model mean, b. BCC-ESM1, c. IPSL-CM6A-LR, d. MPI-ESM-1-2-HAM, e. NorESM2-LM, f. UKESM1-0-LL).

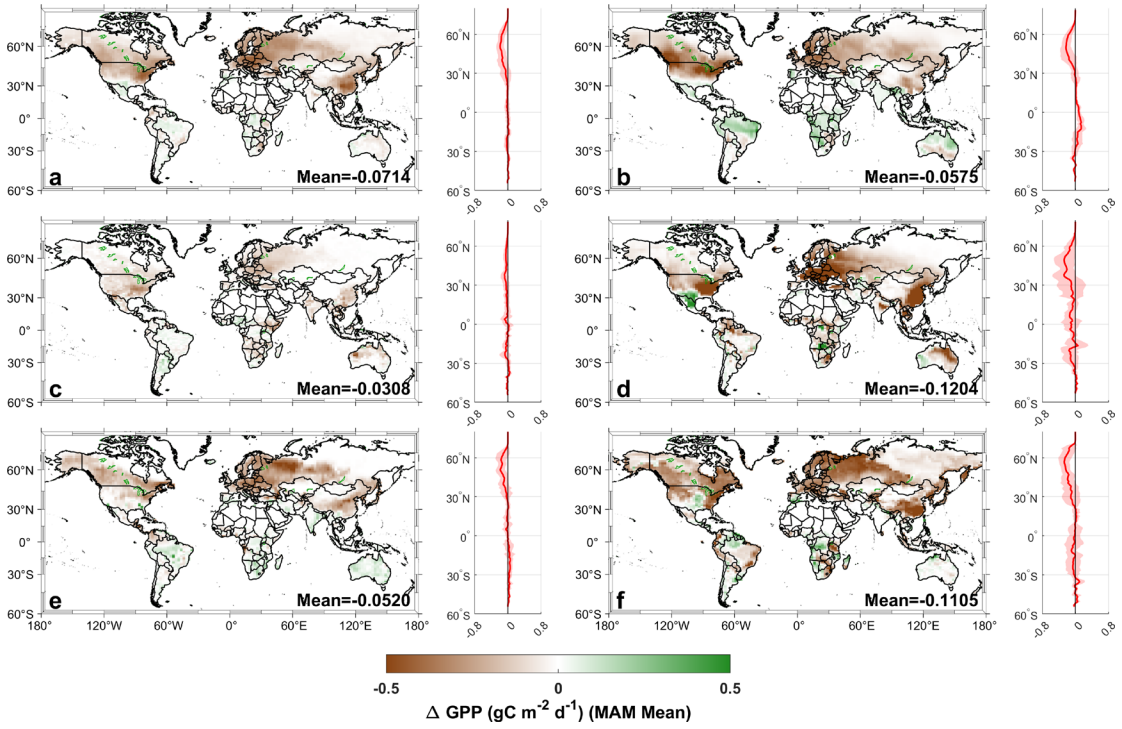

Figure S5. The spatial pattern of changes in ecosystem GPP induced by aerosols from CMIP6 models (a. multi-model mean, b. BCC-ESM1, c. IPSL-CM6A-LR, d. MPI-ESM-1-2-HAM, e. NorESM2-LM, f. UKESM1-0-LL) from March to May.

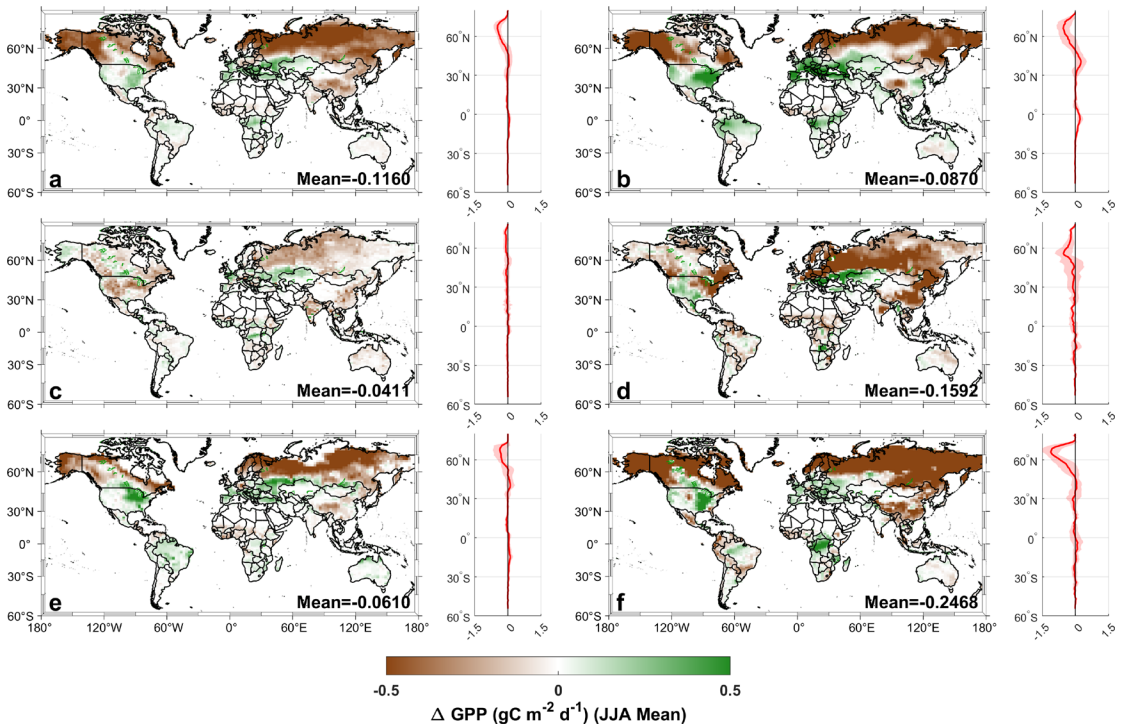

Figure S6. The spatial pattern of changes in ecosystem GPP induced by aerosols from CMIP6 models (a. multi-model mean, b. BCC-ESM1, c. IPSL-CM6A-LR, d. MPI-ESM-1-2-HAM, e. NorESM2-LM, f. UKESM1-0-LL) from June to August.

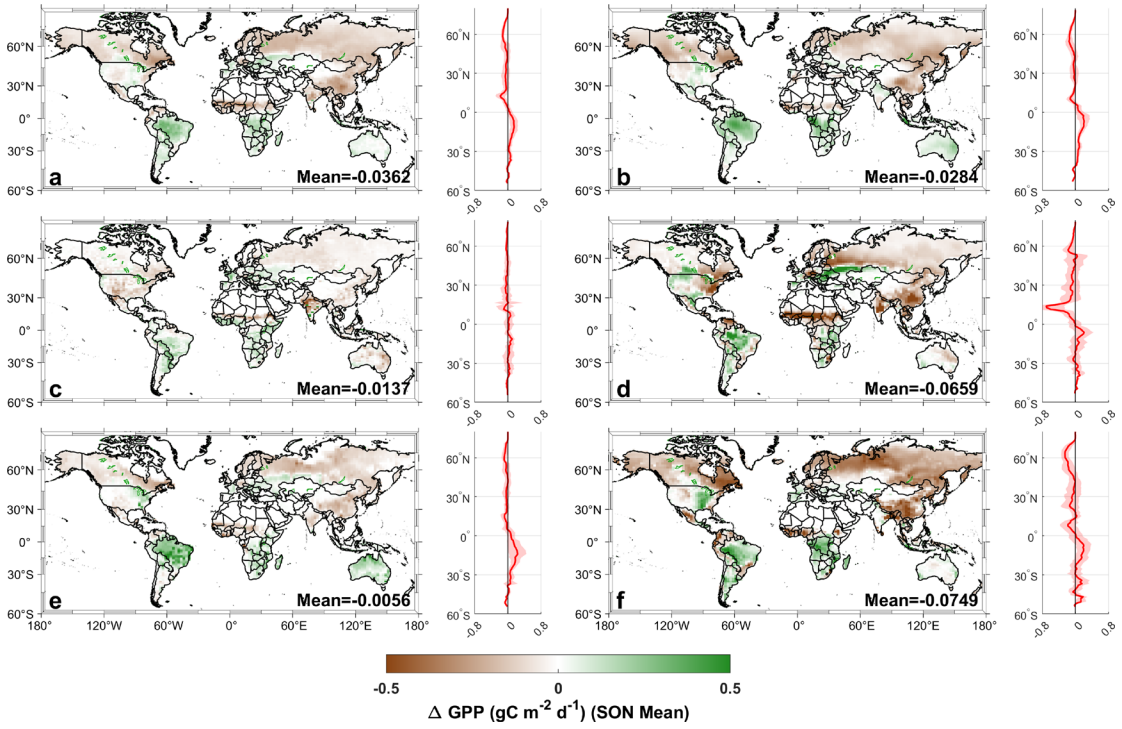

Figure S7. The spatial pattern of changes in ecosystem GPP induced by aerosols from CMIP6 models (a. multi-model mean, b. BCC-ESM1, c. IPSL-CM6A-LR, d. MPI-ESM-1-2-HAM, e. NorESM2-LM, f. UKESM1-0-LL) from September to November.

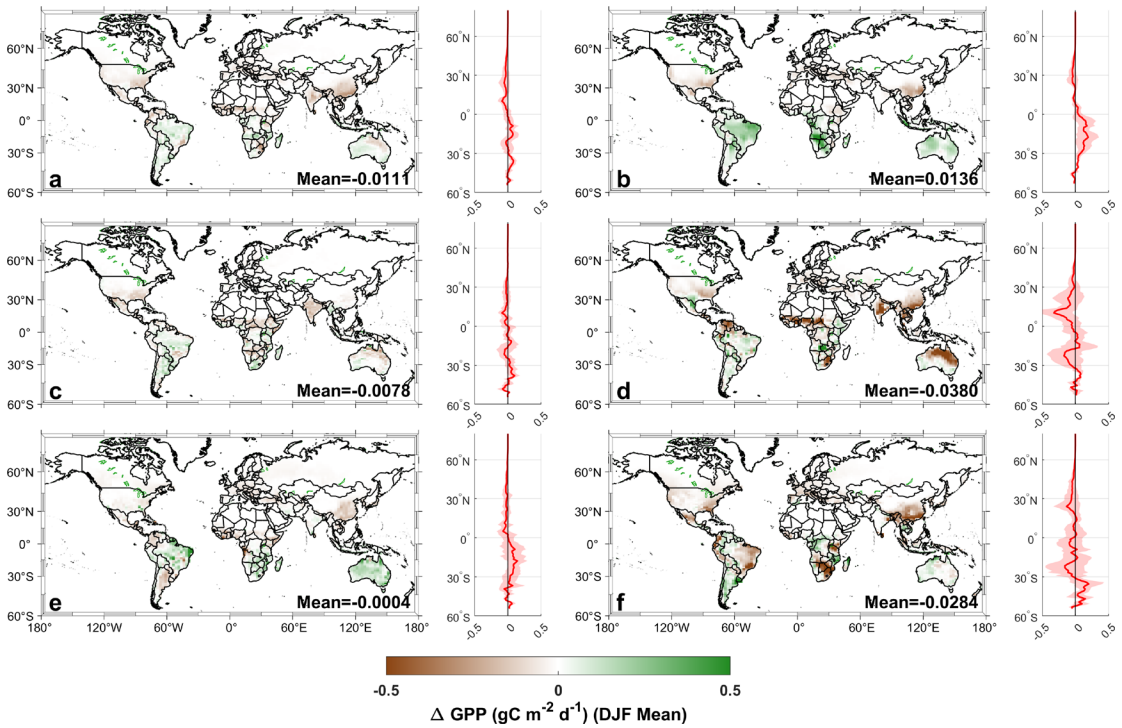

Figure S8. The spatial pattern of changes in ecosystem GPP induced by aerosols from CMIP6 models (a. multi-model mean, b. BCC-ESM1, c. IPSL-CM6A-LR, d. MPI-ESM-1-2-HAM, e. NorESM2-LM, f. UKESM1-0-LL) from December to February.

”

4. Fig. 2: Please provide a second y axis label instead of mixing labels from figures. I think it increases clarity. The same applies to Fig. 1 (and other plots of similar style), I would suggest to give an axis label in all panels and at the bottom of the latitudinal mean side panels to make it straightforward to the reader. It would also be good to put labels with the model names at the top of each panel, and not just in the caption.

Response: Thanks for your comments. We have added the time period and replotted Figure 2. (Please see Figure 2-7)

“

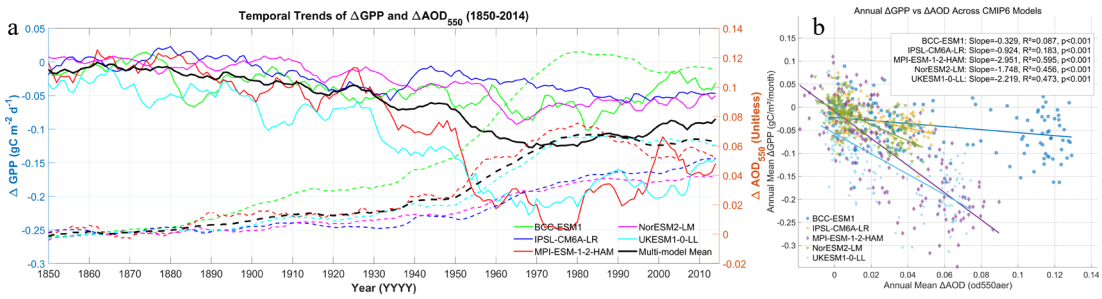

Figure 2. (a) Time series of aerosol-induced GPP changes (solid lines) and AOD variations (dashed lines) from 1850 to 2014 with a ten-years moving window; (b) The scatter plots of annual mean of GPP changes induced by aerosols against the AOD variations.

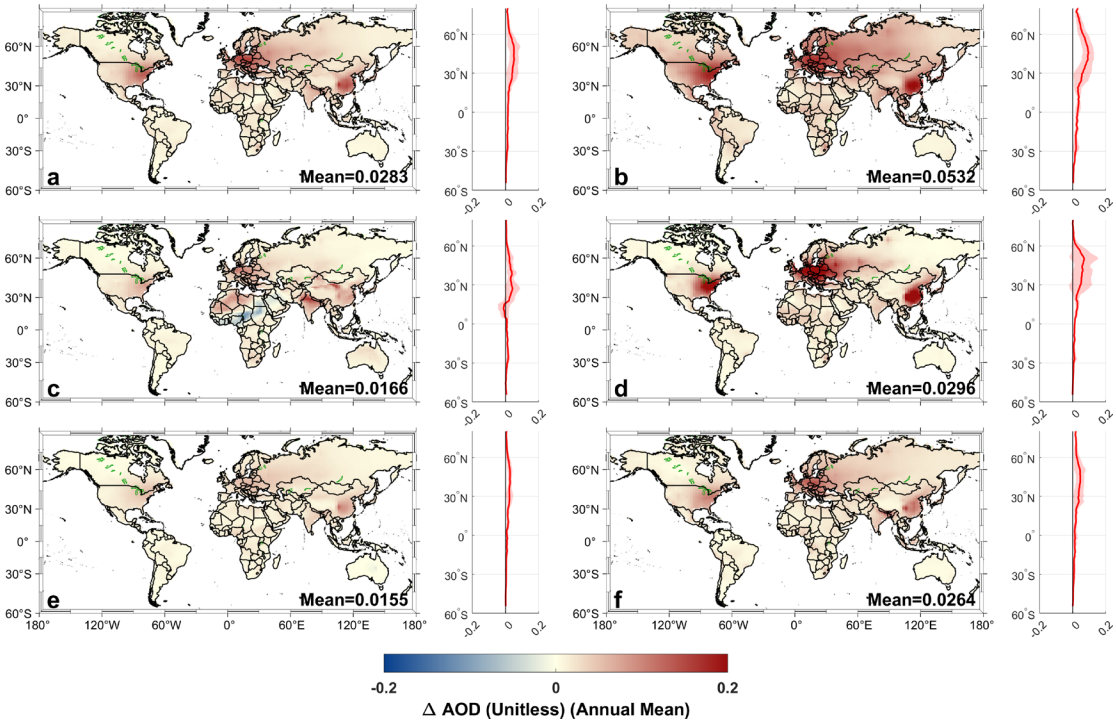

Figure 3. The spatial pattern of mean differences of aerosol optical depth (AOD) at 550nm (od550aer) between historical and hist-piAer experiments over the period 1850–2014 (a. multi-model mean, b. BCC-ESM1, c. IPSL-CM6A-LR, d. MPI-ESM-1-2-HAM, e. NorESM2-LM, f. UKESM1-0-LL).

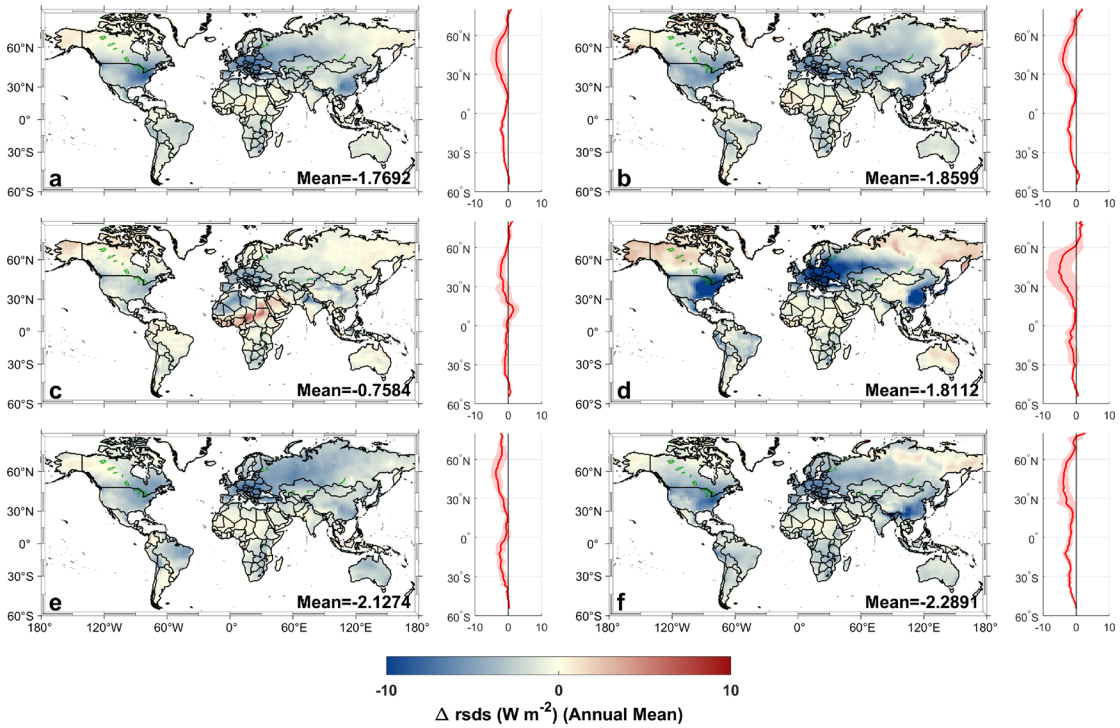

Figure 4. The spatial distribution of mean differences of shortwave radiation (rsds, W/m^2) between historical and hist-piAer experiments from 1850 to 2014 (a. multi-model mean, b. BCC-ESM1, c. IPSL-CM6A-LR, d. MPI-ESM-1-2-HAM, e. NorESM2-LM, f. UKESM1-0-LL).

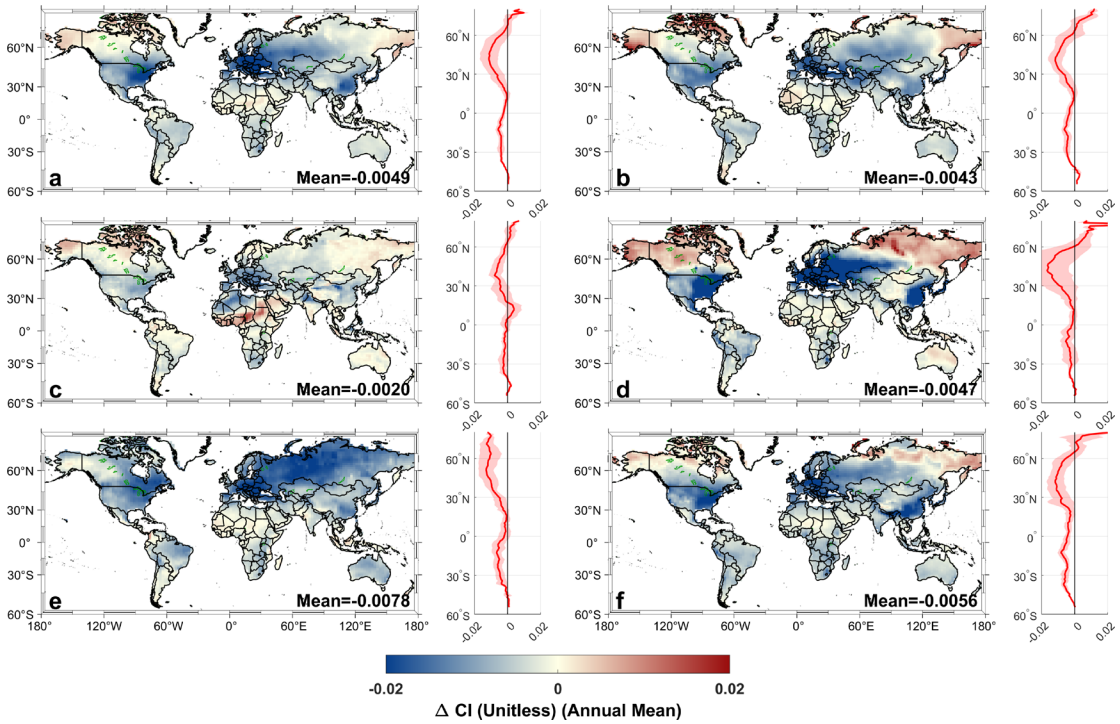

Figure 5. The spatial pattern of mean differences of clearness index (CI) between historical and hist-piAer experiments from 1850 to 2014 (a. multi-model mean, b. BCC-

ESM1, c. IPSL-CM6A-LR, d. MPI-ESM-1-2-HAM, e. NorESM2-LM, f. UKESM1-0-LL).

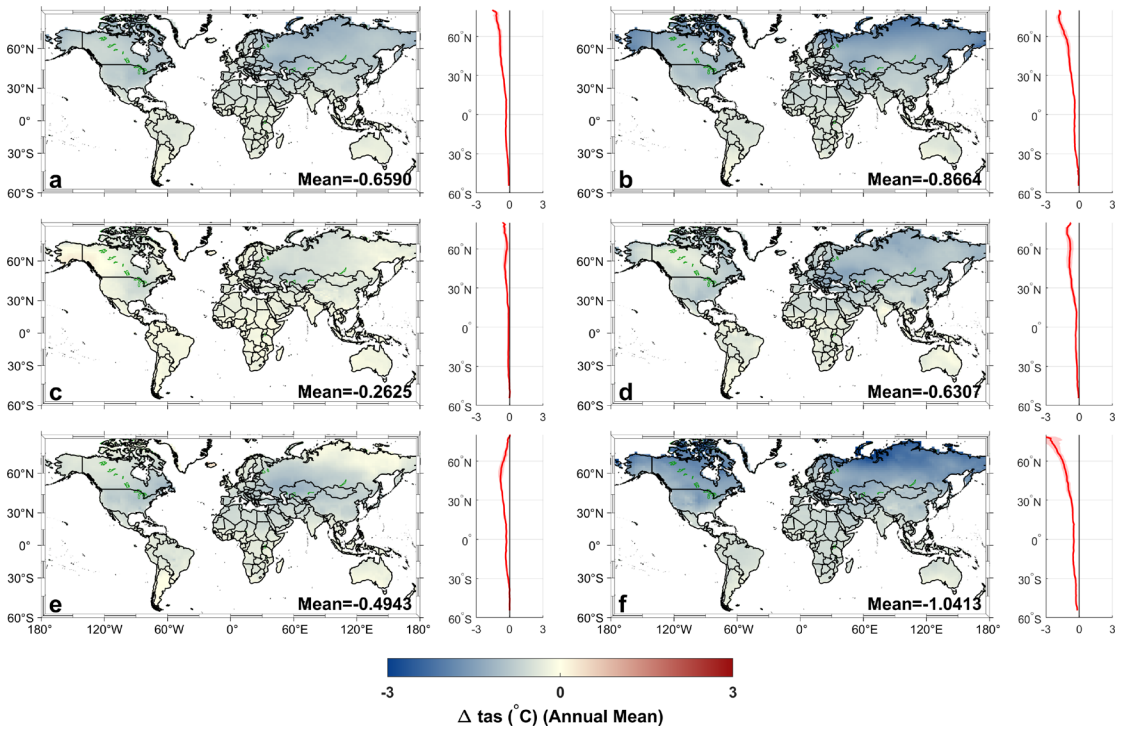

Figure 6. The spatial pattern of mean differences of near-surface air temperature (tas, °C) between historical and hist-piAer experiments from 1850 to 2014 (a. multi-model mean, b. BCC-ESM1, c. IPSL-CM6A-LR, d. MPI-ESM-1-2-HAM, e. NorESM2-LM, f. UKESM1-0-LL).

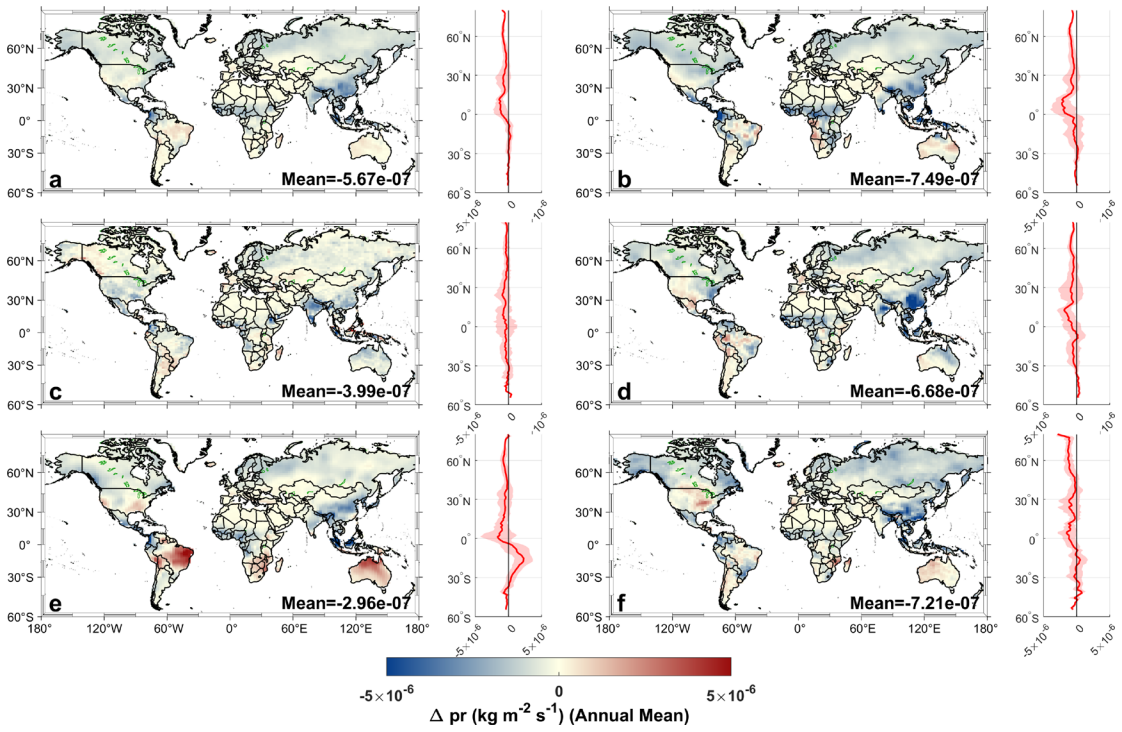

Figure 7. The spatial pattern of mean differences of precipitation (pr, kg/(m^2s)) between historical and hist-piAer experiments from 1850 to 2014 (a. multi-model mean, b. BCC-ESM1, c. IPSL-CM6A-LR, d. MPI-ESM-1-2-HAM, e. NorESM2-LM, f. UKESM1-0-LL).

”

5. L400: Please expand on what you mean with ‘light quality’.

Response: Thanks for the comments. We have added the definition of light quality. (Please see Line 405)

“β_{PAR} and β_{CI} represent the sensitivity of vegetation photosynthesis to light quantity and light quality (light composition and spectral distribution), respectively.”

6. L414-416: You provide a mechanistic link to the vegetation model, which is great. If possible, this would be highly informative for the other sensitivities as well.

Response: Thanks for your comments. In the revised manuscript, we have provided detailed physiological and structural links for the other key sensitivities. (Please see Line 501-503 and Line 425-427)

“The impact of temperature on photosynthesis can be divided into three parts, including chemical limits, adaptation to heat, and phenology.”

“The sensitivity of photosynthesis to precipitation (β_{pr}) links to the soil hydrology schemes and the response of stomatal conductance to water stress.”

7. L491-510: The authors suggest pathways to improve future modelling, but it is not clear based on what they evaluate “accuracy” of any given model? So, either it needs to be clearly presented what they base their conclusion on that “the study suggests

approaches to reduce uncertainty", or this needs to be reformulated in the sense that they identify important mechanisms that need further evaluation.

Response: Thanks for your suggestions. We completely agree with your assessment. Our framework is designed to investigate the sources of inter-model spread. We have modified the sentences related to the model accuracy according to the suggestions. (Please see Line 554-565)

"In this study, our framework identified structural and physiological mechanisms driving the inter-model spread in simulating the response of photosynthesis to aerosols. This also highlights the pathways for future model evaluation and reducing the inter-model spread. First, canopy radiative transfer module should be evaluated to make sure that the model can capture the impacts of diffuse and direct radiation accurately. Some parameters that affect canopy radiation transfer module should be evaluated and incorporated into the model. For example, Li et al. (2023) reported that the light environment within canopy was affected by the clumping index. However, many ESMs do not incorporate the clumping index and this will induce some uncertainties in simulating the canopy light environment (Fang, 2021). Second, the responses of photosynthesis to soil moisture and air temperature require rigorous validation (Gabele et al., 2025)."

References

Bloomfield, K. J., Stocker, B. D., Keenan, T. F., and Prentice, I. C.: Environmental controls on the light use efficiency of terrestrial gross primary production, Global Change Biol, 29, 1037-1053, https://doi.org/10.1111/gcb.16511, 2022.

Fang, H. L.: Canopy clumping index (CI): A review of methods, characteristics, and applications, Agric. For. Meteorol., 303, 108374, https://doi.org/10.1016/j.agrformet.2021.108374, 2021.

Gabele, L. M., Sieber, P., Liu, L., and Seneviratne, S. I.: Soil moisture-induced changes in land carbon sink projections in CMIP6, EGUsphere, 2025, 1-23, https://doi.org/10.5194/egusphere-2025-4215, 2025.

Li, F., Hao, D., Zhu, Q., Yuan, K., Braghiere, R. K., He, L., Luo, X., Wei, S., Riley, W. J., Zeng, Y., and Chen, M.: Vegetation clumping modulates global photosynthesis through adjusting canopy light environment, Glob Chang Biol, 29, 731-746, https://doi.org/10.1111/gcb.16503, 2023.

Shao, L., Li, G., Zhao, Q., Li, Y., Sun, Y., Wang, W., Cai, C., Chen, W., Liu, R., Luo, W., Yin, X., and Lee, X.: The fertilization effect of global dimming on crop yields is not attributed to an improved light interception, Glob Chang Biol, 26, 1697-1713, https://doi.org/10.1111/gcb.14822, 2020.
Song, Y., Jiao, W., Wang, J., and Wang, L.: Increased Global Vegetation Productivity Despite Rising Atmospheric Dryness Over the Last Two Decades, Earth's Future, 10, e2021EF002634, https://doi.org/10.1029/2021ef002634, 2022.
Wang, Z., Chen, W., Piao, J., Cai, Q., Chen, S., Xue, X., and Ma, T.: Synergistic effects of high atmospheric and soil dryness on record-breaking decreases in vegetation productivity over Southwest China in 2023, npj Climate and Atmospheric Science, 8, https://doi.org/10.1038/s41612-025-00895-3, 2025.
Zhang, L., Li, J., Jiang, Z. J., Dong, Y. M., Ying, T., and Zhang, Z. Y.: Clear-Sky Direct Aerosol Radiative Forcing Uncertainty Associated with Aerosol Optical Properties Based on CMIP6 Models, Journal of Climate, 35, 3007-3019, https://doi.org/10.1175/Jcli-D-21-0479.1, 2022.
Zhang, Z. Y., Zhu, K. L., Fan, M., Wang, Q., and Tan, Y. H.: Diffuse Fertilization Effect in Maize and Soybean Is Driven by Improved Light Use Efficiency Rather Than by Light Absorption, J Geophys Res-Biogeo, 129, https://doi.org/10.1029/2023JG007766, 2024.